Biochimie 93 (2011) 1816–1823

Contents lists available at ScienceDirect

Biochimie

journal homepage: www.elsevier.com/locate/biochi

Research paper

Understanding the allosteric trigger for the fructose-1,6-bisphosphate regulation of the ADP-glucose pyrophosphorylase from *Escherichia coli*

Carlos M. Figueroa [a,b,1], María C. Esper [a,1], Ana Bertolo [c], Ana M. Demonte [a], Mabel Aleanzi [a], Alberto A. Iglesias [a], Miguel A. Ballicora [b,*]

[a] Laboratorio de Enzimología Molecular, Instituto de Agrobiotecnología del Litoral (UNL-CONICET), Paraje "El Pozo" CC 242, S3000ZAA Santa Fe, Argentina
[b] Department of Chemistry, Loyola University Chicago, 1068 W Sheridan Rd., Chicago, IL 60660, USA
[c] Department of Plant Biology, Cornell University, Ithaca, NY 14853, USA

ARTICLE INFO

Article history:
Received 21 January 2011
Accepted 24 June 2011
Available online 2 July 2011

Keywords:
Allosteric mechanism
Activation signal propagation
Regulation dynamics
ADP-glucose pyrophosphorylase
Glycogen/starch metabolism

ABSTRACT

ADP-glucose pyrophosphorylase is the enzyme responsible for the regulation of glycogen synthesis in bacteria. The enzyme N-terminal domain has a Rossmann-like fold with three neighbor loops facing the substrate ATP. In the *Escherichia coli* enzyme, one of those loops also faces the regulatory site containing Lys^{39}, a residue involved in binding of the allosteric activator fructose-1,6-bisphosphate and its analog pyridoxal-phosphate. The other two loops contain Trp^{113} and Gln^{74}, respectively, which are highly conserved among all the ADP-glucose pyrophosphorylases. Molecular modeling of the *E. coli* enzyme showed that binding of ATP correlates with conformational changes of the latter two loops, going from an open to a closed (substrate-bound) form. Alanine mutants of Trp^{113} or Gln^{74} did not change apparent affinities for the substrates, but they became insensitive to activation by fructose-1,6-bisphosphate. By capillary electrophoresis we found that the mutant enzymes still bind fructose-1,6-bisphosphate, with similar affinity as the wild type enzyme. Since the mutations did not alter binding of the activator, they must have disrupted the communication between the regulatory and the substrate sites. This agrees with a regulatory mechanism where the interaction with the allosteric activator triggers conformational changes at the level of loops containing residues Trp^{113} and Gln^{74}.

1. Introduction

ADP-glucose pyrophosphorylase (EC 2.7.7.27; ADP-Glc PPase) plays a key role in bacteria and plants catalyzing the rate limiting step of the biosynthesis of reserve polysaccharides, glycogen and starch, respectively (for reviews see [1–5]). A critical feature of this enzyme is that the activity is allosterically modulated by key intermediates of the major carbon and energy metabolism in every studied organism [5]. These effector metabolites are indicators of high or low contents of carbon and energy within the cell, which explains why synthesis of storage polysaccharides in bacteria and plants is enhanced when cellular carbon and energy is in excess [2,3]. For this reason, to properly understand the control of carbon and energy metabolism in these diverse organisms it is critical to unravel the molecular mechanism of the ADP-Glc PPase allosteric regulation. Despite the relatively abundant structural and kinetic information on the ADP-Glc PPase family, the molecular mechanism of the allosteric regulation has been completely unknown thus far.

ADP-Glc PPase catalyzes the formation of ADP-Glc and PP_i from glucose-1P (Glc1P) and ATP. The reaction requires a divalent cation (Mg^{2+}) and, although it is freely reversible *in vitro*, it mainly proceeds in the ADP-Glc synthesis direction within the cell [2,3]. Based on specificity for allosteric regulators, ADP-Glc PPases have been classified in nine different groups [2,3]. For example, in class I, fructose-1,6-bisphosphate (Fru-1,6-P_2) activates the enzyme from enteric bacteria (e.g., *Escherichia coli*), and AMP is an inhibitor [2,3], whereas 3-phosphoglycerate activates the enzyme from plants (class VIII) and orthophosphate is an inhibitor [3]. In all cases, these enzymes are tetramers, but there are differences between bacteria and plants. ADP-Glc PPase from *E. coli* is a homotetramer (α_4), with subunits of ~50 kDa [2], whereas the enzymes from plants are heterotetramers ($\alpha_2\beta_2$) of similar molecular mass [3].

Two ADP-Glc PPase crystallographic structures have been recently solved: a homotetrameric (α_4) form from potato tuber [6]

Abbreviations: ADP-Glc, ADP-glucose; ADP-Glc PPase, ADP-Glc pyrophosphorylase; CZE, capillary zone electrophoresis; Fru-1,6-P_2, fructose-1,6-bisphosphate; Glc1P, glucose-1-phosphate; PLP, pyridoxal-phosphate.

* Corresponding author. Tel.: +1 773 508 3154; fax: +1 773 508 3086.
E-mail address: mballic@luc.edu (M.A. Ballicora).

[1] These authors contributed equally to this work.

0300-9084/$ – see front matter © 2011 Elsevier Masson SAS. All rights reserved.
doi:10.1016/j.biochi.2011.06.029

and the *Agrobacterium tumefaciens* [7] enzyme. In both cases, the three-dimensional structure corresponds to a sulfate-bound, allosterically inhibited form of the enzyme, which has limited the complete understanding of the enzyme's regulatory mechanism [6,7]. Two domains are evident: the N-terminal domain is catalytic and resembles a dinucleotide-binding Rossmann fold, whereas the C-terminal domain is involved in cooperative allosteric regulation and oligomerization [2,6,8–10]. Studies performed by using different experimental approaches have shown the existence of an interaction between both domains [11–14]. Current information suggests that the communication between those two domains is important but no detail has been described at the atomic level.

In this work, we developed a molecular model of the *E. coli* ADP-Glc PPase that strongly suggests a mechanism for propagation of the allosteric activation, in which the hydrogen bond interactions between the loops containing Gln^{74} and Trp^{113} play a critical role. After site-directed mutagenesis of those conserved residues, we obtained enzyme forms defective to activation by Fru-1,6-P_2 despite the fact that the amino acids lie in a region distant from the activator binding domain. Characterization of the mutant enzymes highlights the interaction between catalytic and regulatory regions, and provides important evidence of conformational changes related with the mechanism of allosteric activation.

2. Materials and methods

2.1. Chemicals and enzymes

α-D-[U-^{14}C]Glc1P was purchased from GE Healthcare. Glc1P, ATP, ADP-Glc, Fru-1,6-P_2, and inorganic pyrophosphatase were acquired from Sigma–Aldrich. *Pfu* DNA polymerase was purchased from Stratagene. Ampligase, a thermostable DNA ligase, was from Epicenter. All other reagents were of the highest quality available.

2.2. Site-directed mutagenesis

Site-directed mutagenesis was performed by overlap extension PCR [15]. Plasmid pETEC [11], containing the *E. coli* ADP-Glc PPase gene between *Nde*I and *Sac*I sites, was used as template. The overlapping primers for each mutant are detailed in Table S1. The final PCR products were gel-purified, digested with *Nde*I and *Sac*I, and subcloned to obtain the different pETEC-single mutant plasmids. All the plasmids were fully sequenced to confirm incorporation of only the desired mutation.

The Macromolecular Structure, Sequencing and Synthesis Facility (MS^3F) at Michigan State University performed the synthesis of oligonucleotides and automated DNA sequencing.

2.3. Expression and purification of the wild type and mutant enzymes

Expression of the pETEC (and pETEC-single mutant) plasmid, as well as purification of the different recombinant enzymes was performed as previously described [11]. Briefly, *E. coli* BL21 (DE3) cells were transformed with the pETEC plasmids to express the native and single mutant ADP-Glc PPases. Cells were grown at 37 °C up to OD_{600} ~0.6 and induced with 1 mM IPTG for 4 h at room temperature. After induction, cells were chilled on ice, harvested by centrifugation and stored at −80 °C until use.

All protein purification steps were conducted at 0–4 °C. The cell pastes were resuspended in *buffer A* (50 mM Hepes, pH 8.0, 5 mM $MgCl_2$, 0.1 mM EDTA, and 10% w/v sucrose), disrupted by sonication, and the lysates were cleared by centrifugation. The resulting crude extracts were loaded onto a DEAE-Fractogel column (EMD Chemicals) and eluted with a linear NaCl gradient (0–0.5 M). The active fractions were pooled and precipitated by ammonium sulfate cut (30–60% saturation). The pellet recovered after centrifugation was resuspended in *buffer A* and desalted on Bio-Rad 10 DG chromatography columns equilibrated with the same buffer. The desalted samples were applied to a Mono Q HR 5/5 (FPLC, GE Healthcare) column, equilibrated with *buffer A*, and eluted with a linear NaCl gradient (0–0.5 M). We combined the fractions with highest purity (as determined by SDS-PAGE), after which they were concentrated using Centricon-30 devices (Millipore). By this procedure, the wild type and mutant enzymes reached a purity of ~80%. The purified enzymes were stored at −80 °C until use; conditions where they remained fully active during, at least, three months.

2.4. Protein assay and gel electrophoresis

Protein concentration was alternatively measured by using the bicinchoninic acid reagent [16] or the Bradford method [17]. BSA was utilized as the standard. Protein concentration of the purified enzymes was estimated by the UV absorbance at 280 nm using an extinction coefficient of 1.0 ml mg^{-1} cm^{-1} [18,19]. Protein electrophoresis under denatured conditions (SDS-PAGE) was performed according to Laemmli [20], using the Bio-Rad mini-gel apparatus and 4–15% Tris–HCl pre-cast gradient polyacrylamide gels. Following electrophoresis, protein bands were visualized by staining with Coomasie Brilliant Blue R-250.

2.5. Capillary zone electrophoresis (CZE)

CZE was performed using a SpectraPhoresis 100 (Thermo Separation Products) apparatus. The capillary tubing (Microsolv) was coated with sulfonic groups, with 100 μm internal diameter, a length of 45 cm from the inlet to detector, and a length from the detector to the outlet of 8 cm. Data were collected and analyzed with a RIAC-Processor 2.0 (processing velocity of 10 data/s). Runs were carried out in 50 mM Hepes–NaOH, pH 8.0, at 25 °C, using a voltage of 15 kV, and detection at 220 nm. Hydrocaffeic acid [3-(3,4-dihydroxyphenyl) propionic acid] (Sigma) was used as the running marker. Samples were pressure injected into the capillary for 3 s.

Apparent dissociation constants (K_D') of Fru-1,6-P_2 binding were measured by affinity capillary electrophoresis, where CZE of ADP-Glc PPase was performed in the absence or in the presence of variable concentrations of the allosteric activator. Under these conditions mobility of the enzyme changed as a function of the ligand concentration [21,22]. Changes in electrophoretic migration ($\Delta\mu$) of the enzyme respect to the internal standard were calculated according to the equation [22]:

$$\Delta\mu = [(1/T_{EA})(T_{SA}/T_S)] - (1/T_E),$$

where T_E and T_{EA} are the migration times of the enzyme alone and complexed with the allosteric activator, respectively; and T_S and T_{SA} are the migration times of the internal standard in the absence and in the presence of Fru-1,6-P_2 added to the running buffer, respectively. Values of $\Delta\mu$ were then fitted to a modified Hill equation:

$$\Delta\mu = \Delta\mu_{max}[\text{Fru}-1,6-P_2]^n/([\text{Fru}-1,6-P_2]^n + K_D^{'n}),$$

$\Delta\mu_{max}$ being the maximal relative change in electrophoretic mobility of the enzyme when saturated with the allosteric activator, K_D' the apparent dissociation constant of the complex, and n the Hill number (n_H). Values of K_D' were calculated from data sets acquired at least by triplicate, with repetitions differing by less than ±10%.

2.6. Reductive phospho-pyridoxylation

Wild type and mutant ADP-Glc PPase enzymes were reductively phospho-pyridoxylated in the dark, at room temperature, essentially as previously described [23,24], except that non-radioactive PLP was utilized. The enzymes (about 50 μg/ml) were incubated in 50 mM Hepes–NaOH, pH 8.0, with 10 μM PLP in the presence of 2.5 mM ADP-Glc. After 30 min incubation, $NaBH_4$ was added to a final concentration of 2 mM. The reduction was allowed to proceed for 30 min and then samples were concentrated-desalted using Centricon devices for further analysis of protein concentration, activity and CZE motility.

2.7. Enzyme activity assays

Activity of ADP-Glc PPase was assayed in the direction of ADP-Glc synthesis. The assays were performed at 37 °C and pH 8.0. One unit (U) of enzymatic activity is equal to 1 μmol of product (either ADP-Glc or PPi, as determined by assays A or B, respectively) formed per min under the assay conditions specified below.

Assay A. Synthesis of [^{14}C]ADP-Glc from [^{14}C]Glc1P and ATP was followed by the method of Yep et al. [25]. The reaction was carried out for 10 min in a mixture that contained (unless otherwise specified) 50 mM Hepes, 7 mM $MgCl_2$, 0.5 mM [^{14}C]Glc1P (~1000 dpm/nmol), 1.5 mM ATP, 0.0015 U/μl pyrophosphatase, and 0.2 mg/ml BSA, plus enzyme in a total volume of 200 μl.

Assay B. Synthesis of ADP-Glc was alternatively followed by the high sensitive, colorimetric method developed by Fusari et al. [26]. The standard assay medium was essentially identical as in assay A, except that [^{14}C]Glc1P was replaced by the non-radioactive reagent, Glc1P (also at 0.5 mM final concentration). The reaction was stopped with the addition of Malachite Green color reagent, and read at 650 nm as previously specified [26].

2.8. Kinetic characterization

Kinetic data were plotted as specific activity (μmol min^{-1} mg^{-1}) versus substrate or effector concentration. Kinetic constants were acquired by fitting the data to the Hill equation with a non-linear least-squares formula using the program Origin 7.0 (OriginLab). Hill plots were used to calculate the Hill coefficient (n_H) and the kinetic constants that correspond to maximal velocity (V_{max}) as well as the activator, substrate or inhibitor concentrations giving 50% of the maximal activation ($A_{0.5}$), velocity ($S_{0.5}$), or inhibition ($I_{0.5}$), respectively. Kinetic constants are the mean of at least three independent sets of data, reproducible within ±10%. Sample standard deviations of the data were calculated from the Hill equation fitting by using the Levenberg–Marquardt method [27].

2.9. Homology modeling

Two models of the *E. coli* ADP-Glc PPase (residues 9 to 428) were constructed with the program Modeller 9v2 (http://salilab.org/modeller/) [28]. As templates we used the atomic coordinates of the potato tuber ADP-Glc PPase small subunit chain A, either without ligands (PDB code 1YP2) or complexed with ATP (PDB code 1YP3) [6], and those of the *A. tumefaciens* ADP-Glc PPase (PDB code 3BRK) [7]. Sequence alignment was performed manually to mach functionally conserved residues and predicted secondary structures. The accuracy of the models was assessed with the Verify3D Structure Evaluation Server (http://nihserver.mbi.ucla.edu/Verify_3D/) [29]. Proper orientation of asparagines and glutamines were determined by Molprobity and flipped if needed [30]. Figures were prepared using the Swiss-PdbViewer v3.7 program (http://spdbv.vital-it.ch/) [31].

3. Results

We have recently reported linker scanning mutagenesis studies on the ADP-Glc PPase producing random insertions of a single 15-bp fragment into a recombinant *E. coli glgC* gene [32]. One of the generated mutants, Ec-ins8, had the addition of five amino acids (FKHLL) at one connecting loop of the α–β region that belongs to the Rossmann-like fold of the protein [2,3,6,33]. The insertion specifically occurred between residues Leu^{102} and Pro^{103}, which is in the loop containing a residue (Tyr^{114}) previously identified as important for the binding of ATP to the *E. coli* enzyme [34,35] (Figure S1). However, the distinct kinetic property exhibited by Ec-ins8 was insensitivity to activation by Fru-1,6-P_2, suggesting that this region is also related to regulation [32]. Molecular modeling studies of the *E. coli* ADP-Glc PPase suggested a critical role for that region, where two other neighbor loops with important or conserved residues are located (Fig. 1). Lys^{39} is a residue involved in activator binding [36], Gln^{74} and Trp^{113} are highly conserved (Figure S1), and Tyr^{114} was found to interact with the substrate ATP [34].

As shown in Fig. 2, molecular modeling of *E. coli* ADP-Glc PPase rendered two enzyme structures: one open form with no substrate bound (Fig. 2A) and one closed form (Fig. 2B) with ATP. Remarkably, the open or closed states mainly differ in the region including the loop containing Lys^{39} (involved in the binding of activator) and the two adjacent loops where Gln^{74} and Trp^{113} are localized. In the model of the closed form, the amide group of Gln^{74} links, via hydrogen bonds, the peptide backbones of Arg^{29} and Trp^{113} (Fig. 2B). Arg^{29} is in the Gly rich region proposed as part of the active site [7]. This hydrogen bond network is disrupted by the conformational change that leads to the open form (Fig. 2A). The distances between the atoms involved in the hydrogen bonds in the closed form increased from 3.2 to 6.2 and 2.6 to 7.2 Å, respectively, in the open form. We discarded the possibility that these hydrogen bonds are artifacts of the modeling process because identical interactions are also observed in the crystal structure of the potato tuber enzyme (Fig. 2C) [6]. Thus, the models of the *E. coli* enzyme provide a hypothesis in which the main activation effect of the allosteric ligand Fru-1,6-P_2 is exerted by favoring and/or stabilizing

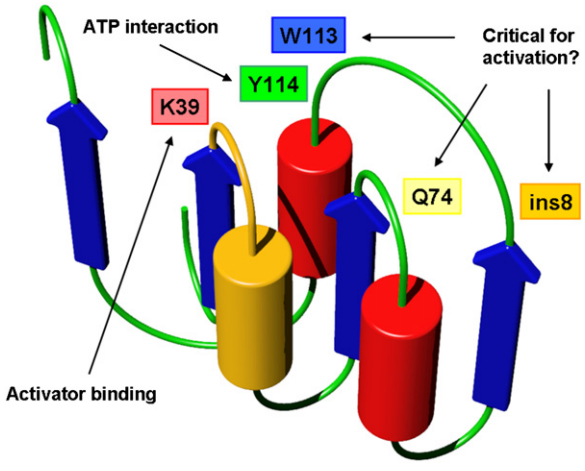

Fig. 1. Three dimensional arrangement of the *E. coli* ADP-Glc PPase N-terminus. Cartoon representation of a model corresponding to the first half (~150 residues) of the Rossmann-like domain. Amino acids involved in ATP (Tyr^{114}) and Fru-1,6-P_2 (Lys^{39}) interaction are highlighted in green and red, respectively. The site of the insertion found in Ec-ins8 is depicted in orange. The highly conserved residues Trp^{113} and Gln^{74} located in loop regions are shown in blue and yellow, respectively. For complementary information, see Figure S1. The model was built as described under "Materials and methods".

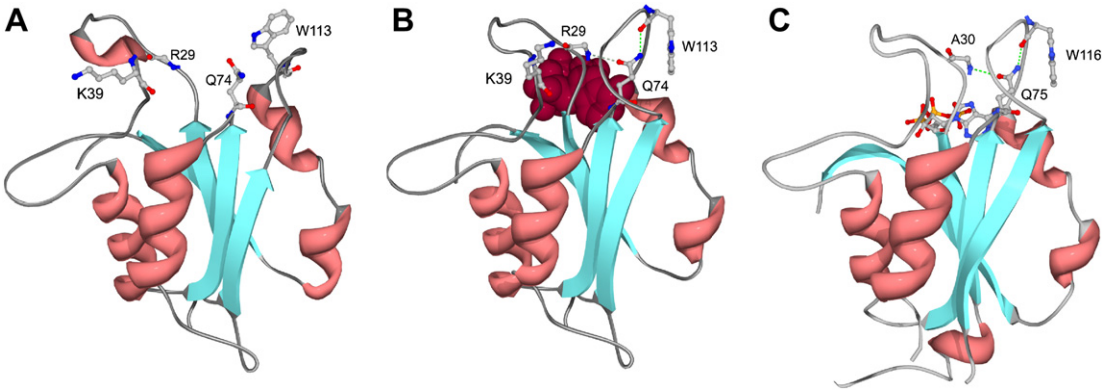

Fig. 2. Homology models of the *E. coli* ADP-Glc PPase alone and with ATP bound. Models show the three dimensional arrangement of the loops studied in the present work and revealed as critical for allosteric regulation. (A) Model for the enzyme alone. (B) Model for the enzyme after binding of the substrate ATP (colored in red as van der Waals radii). Key residues for allosteric regulation are shown together with the hydrogen bonds they form in the closed form of the *E. coli* enzyme. (C) Crystal structure of potato tuber ADP-Glc PPase in complex with ATP (shown as "balls and sticks"). Interactions seen in (B) are also observed in the crystal structure of the potato tuber enzyme. Models were built as described under "Materials and methods".

the closed form of the enzyme, inducing a conformational change from the open form. According to this hypothesis, Gln^{74} anchors a loop important for catalysis and one important for regulation.

To test the above hypothesis, we constructed mutants W113A and Q74A of the ADP-Glc PPase from *E. coli*, expressed them, and determined their kinetic properties. Fig. 3 shows that purified W113A and Q74A mutant enzymes were insensitive to Fru-1,6-P_2 activation, and that the kinetic behavior of these mutants was similar to the Ec-ins8 mutant enzyme [32]. They had almost no activation (1.5-fold) by Fru-1,6-P_2, whereas this effector increased the V_{max} of the wild type enzyme by about 55-fold (Fig. 3). Table 1 gives further evidence that the only significant kinetic difference exhibited by mutants W113A and Q74A, as well as the Ec-ins8 insertion, was insensitivity to the allosteric activator Fru-1,6-P_2. The kinetic parameters for substrates of the wild type ADP-Glc PPase were affected by Fru-1,6-P_2, which increases the affinity for Glc1P (5-fold) and remarkably toward ATP (~35-fold). Conversely, for the mutant enzymes the substrates' $S_{0.5}$ values were not significantly reduced or they were even slightly increased by Fru-1,6-P_2 (Table 1). As a whole, results in Table 1 show that the kinetic

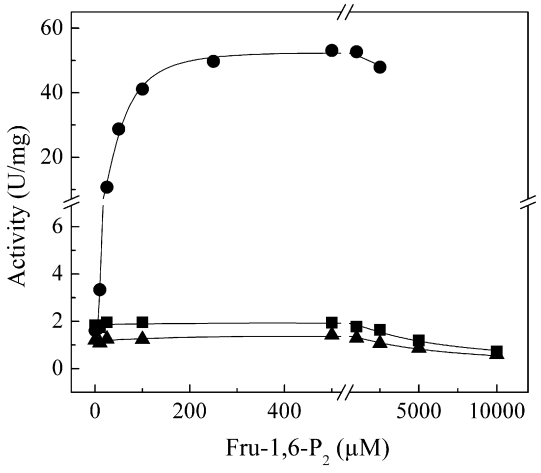

Fig. 3. Insensitivity toward Fru-1,6-P_2 activation of the Q74A and W113A mutant ADP-Glc PPases. Saturation curves for Fru-1,6-P_2 for the wild type (●), Q74A (▲), and W113A (■) enzymes. Assays were performed using Assay A as specified under "Materials and methods", with the variable specified additions of Fru-1,6-P_2. The sample standard deviations for the wild type, Q74A and W113A curves were 1.94, 0.08 and 0.12 U/mg, respectively.

parameters for substrates of both, W113A and Q74A, mutants are quite similar to those found for the wild type enzyme in the absence of the allosteric regulator, and essentially identical to the Ec-ins8 mutant enzyme.

To further explore on the functional relevance played by the physicochemical characteristics of the side chains in positions 113 and 74 we replaced Trp^{113} by Leu or Tyr, and Gln^{74} by Glu or Asn. The mutant enzyme W113L was activated only 3-fold by Fru-1,6-P_2; however, the mutation of Trp^{113} residue to Tyr resulted in an enzyme activated nearly 15-fold (Fig. 4), which approximates to the 55-fold activation of the wild type ADP-Glc PPase. Also, the $A_{0.5}$ for Fru-1,6-P_2 of the mutant W113Y was not significantly different from the wild type (Table S2). This supports the idea that the presence of an aromatic amino acid at this position is important. The mutant Q74E was as insensitive as the Q74A enzyme to Fru-1,6-P_2, whereas Q74N was activated 35-fold, which indicates that an amide group at this position is more important than size at this site for regulation (Fig. 4). The $A_{0.5}$ for Fru-1,6-P_2 of the mutant Q74N slightly increased when compared to the wild type (Table S2).

Additionally, we analyzed the behavior of the W113A and Q74A mutant enzymes respect to regulation by AMP, which is the main inhibitor of the *E. coli* ADP-Glc PPase. There is a cross-talk between the inhibition caused by this metabolite and activation exerted by Fru-1,6-P_2, in a way that AMP is a better inhibitor when the activator is also present [2,3,5,12,13,19,36]. The enhanced inhibitory effect of AMP in the presence of Fru-1,6-P_2 was clear for the wild type but not for the mutant enzymes, as illustrated by Table 2 and derived Figure S2 (note the log scale for activity in the figure). Therefore, the lack of activation explains the modest effect of the inhibitor on W113A and Q74A enzymes. Overall, AMP causes similar inhibition on the wild type and mutant enzymes, and the only apparent difference is an indirect consequence of the absence of Fru-1,6-P_2 activation in the mutants (Table 2 and Figure S2).

To rule out the possibility that the mutations prevented the binding of the activator rather than disrupting the putative communication between the regulatory and active sites, we assayed binding of Fru-1,6-P_2 to wild type, W113A, and Q74A enzymes by capillary zone electrophoresis (CZE) [21,22]. Fig. 5 shows that the CZE profile for the wild type enzyme was different in the absence or in the presence of Fru-1,6-P_2. The lower migration time for the enzyme analyzed in the presence of the activator agrees with the fact that binding of Fru-1,6-P_2 to the enzyme produces a change to a more negative net charge of the activator–protein complex. Fig. 5 also illustrates that both mutant

Table 1
Apparent affinities for substrates of *E. coli* wild type, site-directed and Ec-ins8 mutant ADP-Glc PPases. Reactions were performed using Assay A, as described under "Materials and methods". Data are the mean of three identical and independent experiments ± the mean difference of the triplicates.

Substrate	Fru-1,6-P_2	Wild type		W113A		Q74A		Ec-ins8	
	(mM)	$S_{0.5}$ (mM)	n_H	$S_{0.5}$ (mM)	n_H	$S_{0.5}$ (mM)	n_H	$S_{0.5}$ (mM)	n_H
ATP	0	11 ± 4	1.3	5.8 ± 1.2	1.1	7.6 ± 2.1	1.0	7.2 ± 1.8	1.1
	2	0.32 ± 0.02	2.3	2.5 ± 0.3	1.5	9.8 ± 4.0	1.1	7.1 ± 2.0	1.2
Glc1P	0	0.21 ± 0.05	0.6	0.33 ± 0.07	1.3	0.41 ± 0.08	1.2	0.44 ± 0.07	0.8
	2	0.04 ± 0.01	1.1	0.41 ± 0.04	1.0	0.47 ± 0.07	1.0	0.42 ± 0.02	1.4
Mg^{2+}	0	5.0 ± 0.5	2.0	4.8 ± 0.2	2.2	3.0 ± 0.3	2.4	2.8 ± 0.2	4.3
	2	2.4 ± 0.1	3.6	3.7 ± 0.6	2.5	4.0 ± 0.1	2.3	4.6 ± 0.5	1.9

enzymes exhibited similar CZE profiles between them and compared with the wild type, which indicates that they still bind Fru-1,6-P_2. The interaction of Fru-1,6-P_2 with wild type and mutant ADP-Glc PPases was further evaluated by measuring dissociation constants through affinity capillary electrophoresis. By this procedure, we determined K_D' values of 25 μM (n_H = 1.0), 71 μM (n_H = 1.1), and 80 μM (n_H = 1.2) for the binding of the effector to the wild type, W113A, and Q74A mutant enzymes, respectively. The apparent dissociation constant determined for the wild type enzyme is in good agreement with $A_{0.5}$ values of about 50 μM reported for the *E. coli* ADP-Glc PPase from activation kinetic measurements [2,12,13,19,36] (see also Table S2). Based on binding and kinetic parameters, above 1 mM concentration of Fru-1,6-P_2 the mutant enzymes are saturated with the activator but no activation was detected. These results suggest that what is altered in the W113A and Q74A enzymes is the propagation of the signal after binding of the allosteric regulator to produce activation, rather than the proper interaction of the latter with the protein.

The most dramatic effect observed in the mutant enzymes was the decrease in activation. Interestingly, the Fru-1,6-P_2 binding affinity was 3-fold lower for both the W113A and Q74A mutants when compared to the wild type. According to the concerted model of allosterism [37], it is actually expected that these mutations slightly affect the K_D' for the activator, even if the only role of the mutated residues was to trigger the activation without a direct interaction with the ligand. To explain this behavior, we developed a simplified scheme in which there are two enzyme forms, an active closed form and a less active and open form (R and T, respectively, according to the concerted model nomenclature [37]). The activator (A) binds to the R form to yield a RA complex, and also to the T form to yield a TA complex, but with much less affinity (Scheme S1). The K_D' of the wild type enzyme is determined by all the bound species (TA and RA complexes). In our model, for the mutants where the activation was abolished (i.e., disrupted the transition from T to R), the K_D' will be only determined by the binding of the activator to the T form. Then, the ratio between the K_D' for the mutants and the wild type should be given by $1 + 1/L'$, where L' is the equilibrium constant between forms TA and RA (Scheme S1). The ratio we observed, which was ~3 (71 and 80 μM for the W113A and Q74A mutants, respectively, and 25 μM for the wild type) could be easily explained by an L' value of ~0.5, which implies that the closed and open forms in saturated concentration of activator might still be in a dynamic equilibrium (2/3 as RA and 1/3 as TA forms).

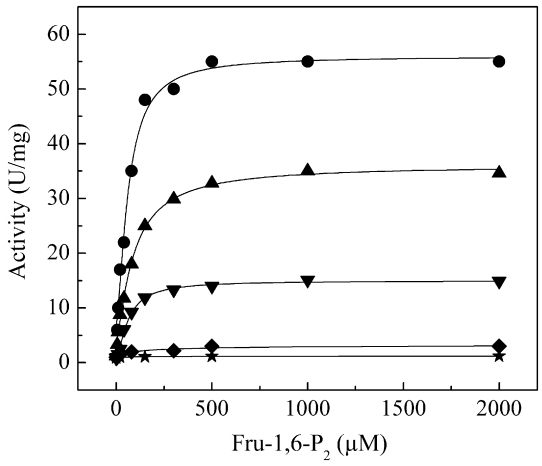

Fig. 4. Different responses to Fru-1,6-P_2 of mutant ADP-Glc PPases having variable characteristic mutated residues. Activation by Fru-1,6-P_2 was analyzed for the wild type (●), and mutant enzymes W113L (◆), W113Y (▼), Q74E (★), and Q74N (▲). The activity of the enzymes was determined using Assay A as described under "Materials and methods". The sample standard deviations for the wild type, W113L, W113Y, Q74E and Q74N curves were 2.16, 0.25, 0.35, 0.003 and 0.82 U/mg, respectively.

In addition, W113A, Q74A, as well as the Ec-ins8 enzymes, exhibited no response to pyridoxal-phosphate (PLP), which is an analogue of Fru-1,6-P_2. Early chemical modification experiments of the *E. coli* ADP-Glc PPase with PLP identified Lys^{39} as involved in activator binding [23,24]. As previously reported [19], when present in the assay medium PLP activated the wild type enzyme to the same degree and with higher affinity than Fru-1,6-P_2; however, it failed to affect the activity of the W113A and Q74A mutants (Fig. 6). At low concentrations, PLP can be covalently linked by reduction with $NaBH_4$, thus modifying a residue involved in activator binding (Lys^{39}) [23,24]. We performed reductive phospho-pyridoxylation of the wild type as well as the W113A and Q74A enzymes under conditions to specifically modify Lys^{39}. The wild type ADP-Glc PPase phospho-pyridoxylated migrated faster in CZE because of a more negative charge (Fig. 7), and in agreement with previous reports [23,24] this form of the enzyme was more active and less sensitive to further activation by Fru-1,6-P_2 (Table 3). Interestingly, after reductive phospho-pyridoxylation, both mutants (W113A and Q74A) migrated faster in CZE (Fig. 7), but they exhibited no significant changes in activity (Table 3). This strongly supports the model in which the mutant enzymes have altered the translation of the regulatory signal, as they can be covalently modified by PLP at Lys^{39} but this binding is ineffective in terms of activation.

Table 2
Effect of AMP and Fru-1,6-P_2 on the activity of *E. coli* wild type, site-directed and Ec-ins8 mutant ADP-Glc PPases. Activity was determined using Assay A at standard concentrations of substrates as detailed under "Materials and methods", without further additions or in the presence of the stated concentrations of AMP and/or Fru-1,6-P_2. Data are the mean of two identical and independent experiments ± the mean difference of the duplicates.

Effector	Activity (U/mg)			
	Wild type	W113A	Q74A	Ec-ins8
Control	1.08 ± 0.12	1.45 ± 0.05	1.93 ± 0.02	0.49 ± 0.01
AMP 0.5 mM	0.72 ± 0.11	0.63 ± 0.05	1.05 ± 0.08	0.32 ± 0.03
Fru-1,6-P_2 2.5 mM	47.6 ± 1.30	1.12 ± 0.09	1.60 ± 0.08	0.43 ± 0.05
AMP 0.5 mM + Fru-1,6-P_2 2.5 mM	3.60 ± 0.18	0.61 ± 0.03	0.82 ± 0.02	0.34 ± 0.01

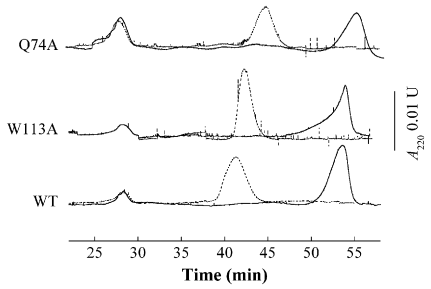

Fig. 5. Electropherograms of wild type and mutant Q74A and W113A ADP-Glc PPases. The wild type, mutant W113A, and mutant Q74A enzymes were run in CZE as specified under "Materials and methods" in the absence (solid lines) or in the presence (dashed lines) of 2.5 mM Fru-1,6-P_2. Small peaks appearing before 30 min correspond to hydrocaffeic acid used as a running marker.

4. Discussion

Many pioneer studies established key structure to function relationships between ADP-Glc PPases from different sources. Those identified distinct domains involved in the binding of substrates [34,35,38], allosteric effectors [19,23,24,36,39], as well as critical residues for catalysis [33,38]. The recent crystallographic resolution of the homotetrameric ADP-Glc PPases from potato tuber [6] and *A. tumefaciens* [7] provided key information about the different domains involved in enzyme activity and regulation. The enzyme has two major domains: a catalytic N-terminal α/β region, and a C-terminal β-helix domain, characteristic of this regulatory pyrophosphorylase. In addition, the tight interaction between the N- and C-terminal domains is critical for determining specificity and affinity for the allosteric activator [11–13]. However, the specific inter-domain interactions that determine the allosteric effect have never been established.

In the present study we identified a dynamic mechanism for the allosteric regulation of the *E. coli* ADP-Glc PPase, in which the propagation of the allosteric signal involves three loops adjacently located in the three dimensional structure of the enzyme. Using models of the *E. coli* enzyme we hypothesized that binding of the activator in a loop located near the N-terminus stabilizes an active conformation facilitating the relative movement of another loop from an open to a closed state. The first loop includes Lys^{39}, which is an activator binding residue [23,24,36], together with other

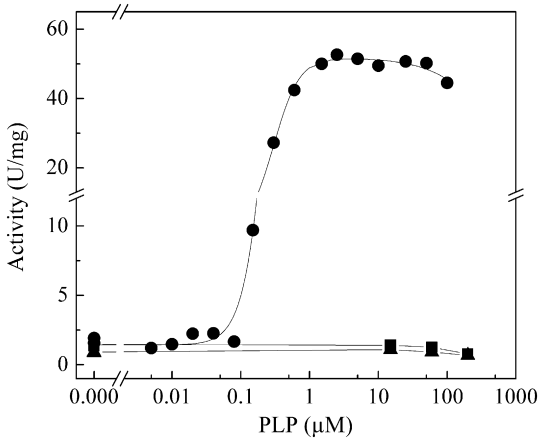

Fig. 6. Different sensitivity to activation by PLP of the wild type and mutant ADP-Glc PPases. Activity assays in the ADP-Glc synthesis direction were performed with the addition of the specified concentrations of PLP for the wild type (●), Q74A (▲), and W113A (■) enzymes. Determinations of enzyme activity were done using Assay A, as described under "Materials and Methods". The sample standard deviations for the wild type, Q74A and W113A curves were 1.88, 0.08 and 0.11 U/mg, respectively.

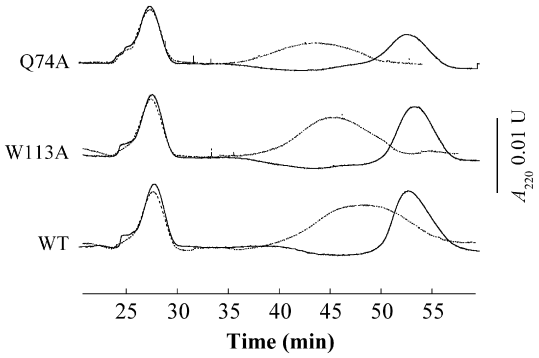

Fig. 7. Different CZE motility of ADP-Glc PPases modified by PLP. The wild type and mutant enzymes were analyzed by CZE in their native state (solid lines) or after reductive phospho-pyridoxylation (dashed lines). The latter modification treatment was performed as detailed under "Materials and methods".

arginine important for regulation [39], and the second one contains Tyr^{114}, which is involved in ATP binding [34,35]. It can be visualized that the binding of the activator to Lys^{39} could promote the formation and stabilization of the closed conformation. Thus, the regulation of the enzyme would be determined by positioning of loops, where a conformational change induced by the substrates and facilitated by the activator turns the open form to a more active closed conformation. These two loops hypothesized to be involved in allosteric activation are interfaced by a third loop in which Gln^{74} is present. This residue is absolutely conserved in all ADP-Glc PPases known so far and must play a critical role in facilitating the communication between the loops through hydrogen bonding. This type of mechanism has been observed in other enzymes [40–42], as a closed arrangement of loops approximates substrates and catalytic residues, conferring key features to an environment suitable for productive catalysis.

This hypothesis was tested by site-directed mutagenesis of the *E. coli* ADP-Glc PPase. Replacing Gln^{74} to Ala^{74}, which has a side chain that cannot form hydrogen bonds, yields an enzyme completely insensitive to activation (Fig. 3). Moreover, the low affinity for ATP of this mutant is similar to the one observed with the wild type enzyme in absence of activator (Table 1). Since the binding of activator Fru-1,6-P_2 was confirmed by CZE (Fig. 5), the communication between the loops must have been disrupted. In fact, the importance of hydrogen bonds of Gln^{74} was confirmed by Asn replacement, as it was substantially sensitive to activation, unlike the Ala mutant (Fig. 4). The Asn residue is one methylene shorter than Gln, but is still capable of forming two hydrogen bonds. On the other hand, mutation to Glu, which can accept a H-bond but cannot donate one at a neutral pH, renders an enzyme form that is insensitive to activation (Fig. 4). The N of the Gln^{74} side chain donates a hydrogen bond to the backbone oxygen of the

Table 3
Activity and response to Fru-1,6-P_2 of *E. coli* wild type and mutant ADP-Glc PPases before and after reductive phospho-pyridoxylation. The wild type and mutant enzymes were reductively phospho-pyridoxylated as specified under "Materials and methods" and their activity was determined using Assay B. Data are the mean of two identical and independent experiments ± the mean difference of the duplicates.

Modification		Wild type	W113A	Q74A
None	Activity (U/mg)	1.4 ± 0.5	1.2 ± 0.3	3.1 ± 0.5
	Activity + Fru-1, 6-P_2 (U/mg)	63 ± 10	1.9 ± 0.3	3.8 ± 0.5
	Activation (fold)	44	1.6	1.2
Reductive pyridoxylation	Activity (U/mg)	12 ± 2	0.87 ± 0.02	1.6 ± 0.1
	Activity + Fru-1, 6-P_2 (U/mg)	49 ± 5	1.2 ± 0.5	1.7 ± 0.2
	Activation (fold)	4.1	1.4	1.1

highly conserved Trp^{113}. Replacement of the side chain in position 113 should not interfere in the hydrogen bond formation since the acceptor is an atom of the backbone. However, mutation of Trp^{113} to Ala^{113} also abolishes the sensitivity to activation (Fig. 3). A bulky hydrophobic residue (Leu) cannot effectively replace Trp, but an aromatic one (Tyr) could partially do it. Therefore, the importance of this Trp^{113} may be related to its aromatic ring. We postulate that the role of Trp^{113} is to anchor the loop in a conformation where the backbone can interact with Gln^{74}. Molecular dynamic experiments to prove this hypothesis are underway. In other tetrameric enzymes, it was proposed that the transition from open to closed conformations not only induces an increase in catalytic activity of one subunit, but also could drive an inter-subunit signal that stabilizes a general activated state in the whole tetramer [41–43]. It was observed in the crystal structure of the ADP-Glc PPase from potato tuber that the loop containing the homologous version of Trp^{113} is near the inter-subunit interface [6]. It is certainly possible that this allosteric signal will propagate through the whole tetramer.

The roles of conformational changes and motion in proteins are gaining momentum, because of the relevance they have for enzyme catalysis and allosteric regulation [42–48]. The current view is that proteins are in constant motion [49] and that intrinsic dynamic properties are responsible for signaling and allostery [43,47]. Protein dynamics include conformational changes involving two main processes: domain motion, where two rigid domains joined by a flexible hinge move relative to each other; and loop motion, meaning the movement of flexible loop surface to different conformations [45]. These conformational changes are triggered by binding of substrates or allosteric effectors and they fulfill different roles in catalysis, mainly orienting groups to favor binding and positioning of substrates as well as removal of water and trapping of activated intermediates [42,45,46,48]. Here, we propose a regulatory mechanism in which the interaction of the allosteric activator with the enzyme communicates the regulatory signal through conformational changes of loops containing the residues Trp^{113} and Gln^{74}. This is a universally conserved motif present in all ADP-Glc PPases, even in the ones with different allosteric properties and very low sequence identity. For that reason, it is tempting to speculate that this family of enzymes may have a common allosteric trigger that links a conserved catalytic site to a divergent allosteric site. This may be a very effective evolutionary mechanism to activate metabolically diverse enzymes.

Acknowledgements

CMF is a Postdoctoral Fellow from CONICET and AAI is a Principal Investigator from the same Institution. AAI is a Fellow from The John Simon Guggenheim Memorial Foundation, and CMF is a recipient of a Fulbright Fellowship. This work was supported by grants to AAI from CONICET [PIP 2519], UNL [CAI + D Orientado and Redes], and ANPCyT [PICT'08 1754]; and to MAB from the National Science Foundation [grant MCB 1024945].

Appendix. Supplementary data

Supplementary data associated with this article can be found in the online version, at doi:10.1016/j.biochi.2011.06.029.

References

[1] S.G. Ball, M.K. Morell, From bacterial glycogen to starch: understanding the biogenesis of the plant starch granule, Annu. Rev. Plant Biol. 54 (2003) 207–233.
[2] M.A. Ballicora, A.A. Iglesias, J. Preiss, ADP-glucose pyrophosphorylase, a regulatory enzyme for bacterial glycogen synthesis, Microbiol. Mol. Biol. Rev. 67 (2003) 213–225.
[3] M.A. Ballicora, A.A. Iglesias, J. Preiss, ADP-glucose pyrophosphorylase: a regulatory enzyme for plant starch synthesis, Photosyn. Res. 79 (2004) 1–24.
[4] A.A. Iglesias, J. Preiss, Bacterial glycogen and plant starch biosynthesis, Biochem. Educ. 20 (1992) 196–203.
[5] M.N. Sivak, J. Preiss, Starch: basic science to biotechnology. in: S.L. Taylor (Ed.), Advances in Food and Nutrition Research. Academic Press, San Diego, 1998, pp. 1–199.
[6] X. Jin, M.A. Ballicora, J. Preiss, J.H. Geiger, Crystal structure of potato tuber ADP-glucose pyrophosphorylase, Embo J. 24 (2005) 694–704.
[7] J.R. Cupp-Vickery, R.Y. Igarashi, M. Perez, M. Poland, C.R. Meyer, Structural analysis of ADP-glucose pyrophosphorylase from the bacterium *Agrobacterium tumefaciens*, Biochemistry 47 (2008) 4439–4451.
[8] I. Baris, A. Tuncel, N. Ozber, O. Keskin, I.H. Kavakli, Investigation of the interaction between the large and small subunits of potato ADP-glucose pyrophosphorylase, PLoS Comput. Biol. 5 (2009) e1000546.
[9] S.K. Boehlein, J.R. Shaw, J.D. Stewart, L.C. Hannah, Characterization of an autonomously activated plant ADP-glucose pyrophosphorylase, Plant Physiol. 149 (2009) 318–326.
[10] N. Georgelis, J.R. Shaw, L.C. Hannah, Phylogenetic analysis of ADP-glucose pyrophosphorylase subunits reveals a role of subunit interfaces in the allosteric properties of the enzyme, Plant Physiol. 151 (2009) 67–77.
[11] M.A. Ballicora, J.I. Sesma, A.A. Iglesias, J. Preiss, Characterization of chimeric ADPglucose pyrophosphorylases of *Escherichia coli* and *Agrobacterium tumefaciens*. Importance of the C-terminus on the selectivity for allosteric regulators, Biochemistry 41 (2002) 9431–9437.
[12] C.M. Bejar, M.A. Ballicora, D.F. Gomez-Casati, A.A. Iglesias, J. Preiss, The ADP-glucose pyrophosphorylase from Escherichia coli comprises two tightly bound distinct domains, FEBS Lett. 573 (2004) 99–104.
[13] C.M. Bejar, M.A. Ballicora, A.A. Iglesias, J. Preiss, ADPglucose pyrophosphorylase's N-terminus: structural role in allosteric regulation, Biochem. Biophys. Res. Commun. 343 (2006) 216–221.
[14] S.K. Boehlein, A.K. Sewell, J. Cross, J.D. Stewart, L.C. Hannah, Purification and characterization of adenosine diphosphate glucose pyrophosphorylase from maize/potato mosaics, Plant Physiol. 138 (2005) 1552–1562.
[15] S.N. Ho, H.D. Hunt, R.M. Horton, J.K. Pullen, L.R. Pease, Site-directed mutagenesis by overlap extension using the polymerase chain reaction, Gene 77 (1989) 51–59.
[16] P.K. Smith, R.I. Krohn, G.T. Hermanson, A.K. Mallia, F.H. Gartner, M.D. Provenzano, E.K. Fujimoto, N.M. Goeke, B.J. Olson, D.C. Klenk, Measurement of protein using bicinchoninic acid, Anal. Biochem. 150 (1985) 76–85.
[17] M.M. Bradford, A rapid and sensitive method for the quantitation of microgram quantities of protein utilizing the principle of protein-dye binding, Anal. Biochem. 72 (1976) 248–254.
[18] Y.Y. Charng, A.A. Iglesias, J. Preiss, Structure-function relationships of cyanobacterial ADP-glucose pyrophosphorylase. Site-directed mutagenesis and chemical modification of the activator-binding sites of ADP-glucose pyrophosphorylase from Anabaena PCC 7120, J. Biol. Chem. 269 (1994) 24107–24113.
[19] T. Haugen, A. Ishaque, J. Preiss, ADPGlucose pyrophosphorylase: evidence for a lysine residue at the activator site of the *Escherichia coli* B enzyme, Biochem. Biophys. Res. Commun. 69 (1976) 346–353.
[20] U.K. Laemmli, Cleavage of structural proteins during the assembly of the head of bacteriophage T4, Nature 227 (1970) 680–685.
[21] J. Kaddis, C. Zurita, J. Moran, M. Borra, N. Polder, C.R. Meyer, F.A. Gomez, Estimation of binding constants for the substrate and activator of Rhodobacter sphaeroides adenosine 5′-diphosphate-glucose pyrophosphorylase using affinity capillary electrophoresis, Anal. Biochem. 327 (2004) 252–260.
[22] G. Li, X. Zhou, Y. Wang, A. El-Shafey, N.H. Chiu, I.S. Krull, Capillary isoelectric focusing and affinity capillary electrophoresis approaches for the determination of binding constants for antibodies to the prion protein, J. Chromatogr. A 1053 (2004) 253–262.
[23] T.F. Parsons, J. Preiss, Biosynthesis of bacterial glycogen. Isolation and characterization of the pyridoxal-P allosteric activator site and the ADP-glucose-protected pyridoxal-P binding site of *Escherichia coli* B ADP-glucose synthase, J. Biol. Chem. 253 (1978) 7638–7645.
[24] T.F. Parsons, J. Preiss, Biosynthesis of bacterial glycogen. Incorporation of pyridoxal phosphate into the allosteric activator site and an ADP-glucose-protected pyridoxal phosphate binding site of *Escherichia coli* B ADP-glucose synthase, J. Biol. Chem. 253 (1978) 6197–6202.
[25] A. Yep, C.M. Bejar, M.A. Ballicora, J.R. Dubay, A.A. Iglesias, J. Preiss, An assay for adenosine 5′-diphosphate (ADP)-glucose pyrophosphorylase that measures the synthesis of radioactive ADP-glucose with glycogen synthase, Anal. Biochem. 324 (2004) 52–59.
[26] C. Fusari, A.M. Demonte, C.M. Figueroa, M. Aleanzi, A.A. Iglesias, A colorimetric method for the assay of ADP-glucose pyrophosphorylase, Anal. Biochem. 352 (2006) 145–147.
[27] W.H. Press, B.P. Flannery, S.A. Teukolsky, W.T. Vetterling, Numerical Recipes in C: The Art of Scientific Computing. Cambridge University Press, New York, 1988.
[28] A. Sali, T.L. Blundell, Comparative protein modelling by satisfaction of spatial restraints, J. Mol. Biol. 234 (1993) 779–815.
[29] R. Luthy, J.U. Bowie, D. Eisenberg, Assessment of protein models with three-dimensional profiles, Nature 356 (1992) 83–85.

[30] I.W. Davis, A. Leaver-Fay, V.B. Chen, J.N. Block, G.J. Kapral, X. Wang, L.W. Murray, W.B. Arendall 3rd, J. Snoeyink, J.S. Richardson, D.C. Richardson, MolProbity: all-atom contacts and structure validation for proteins and nucleic acids, Nucleic Acids Res. 35 (2007) W375–W383.
[31] N. Guex, M.C. Peitsch, SWISS-MODEL and the Swiss-PdbViewer: an environment for comparative protein modeling, Electrophoresis 18 (1997) 2714–2723.
[32] M.A. Ballicora, E.D. Erben, T. Yazaki, A.L. Bertolo, A.M. Demonte, J.R. Schmidt, M. Aleanzi, C.M. Bejar, C.M. Figueroa, C.M. Fusari, A.A. Iglesias, J. Preiss, Identification of regions critically affecting kinetics and allosteric regulation of the *Escherichia coli* ADP-glucose pyrophosphorylase by modeling and pentapeptide-scanning mutagenesis, J. Bacteriol. 189 (2007) 5325–5333.
[33] J.B. Frueauf, M.A. Ballicora, J. Preiss, Aspartate residue 142 is important for catalysis by ADP-glucose pyrophosphorylase from *Escherichia coli*, J. Biol. Chem. 276 (2001) 46319–46325.
[34] A. Kumar, T. Tanaka, Y.M. Lee, J. Preiss, Biosynthesis of bacterial glycogen. Use of site-directed mutagenesis to probe the role of tyrosine 114 in the catalytic mechanism of ADP-glucose synthetase from Escherichia coli, J. Biol. Chem. 263 (1988) 14634–14639.
[35] Y.M. Lee, J. Preiss, Covalent modification of substrate-binding sites of *Escherichia coli* ADP-glucose synthetase. Isolation and structural characterization of 8-azido-ADP-glucose-incorporated peptides, J. Biol. Chem. 261 (1986) 1058–1064.
[36] A. Gardiol, J. Preiss, *Escherichia coli* E-39 ADPglucose synthetase has different activation kinetics from the wild-type allosteric enzyme, Arch. Biochem. Biophys. 280 (1990) 175–180.
[37] J. Monod, J. Wyman, J.-P. Changeux, On the nature of allosteric transitions: a plausible model, J. Mol. Biol. 12 (1965) 88–118.
[38] C.M. Bejar, X. Jin, M.A. Ballicora, J. Preiss, Molecular architecture of the glucose 1-phosphate site in ADP-glucose pyrophosphorylases, J. Biol. Chem. 281 (2006) 40473–40484.
[39] D.F. Gomez-Casati, R.Y. Igarashi, C.N. Berger, M.E. Brandt, A.A. Iglesias, C.R. Meyer, Identification of functionally important amino-terminal arginines of *Agrobacterium tumefaciens* ADP-glucose pyrophosphorylase by alanine scanning mutagenesis, Biochemistry 40 (2001) 10169–10178.
[40] D. Datta, J.M. Scheer, M.J. Romanowski, J.A. Wells, An allosteric circuit in caspase-1, J. Mol. Biol. 381 (2008) 1157–1167.
[41] A. del Sol, C.J. Tsai, B. Ma, R. Nussinov, The origin of allosteric functional modulation: multiple pre-existing pathways, Structure 17 (2009) 1042–1050.
[42] S. Raboni, S. Bettati, A. Mozzarelli, Identification of the geometric requirements for allosteric communication between the alpha- and beta-subunits of tryptophan synthase, J. Biol. Chem. 280 (2005) 13450–13456.
[43] R.G. Smock, L.M. Gierasch, Sending signals dynamically, Science 324 (2009) 198–203.
[44] A. Gutteridge, J. Thornton, Conformational change in substrate binding, catalysis and product release: an open and shut case? FEBS Lett. 567 (2004) 67–73.
[45] A. Gutteridge, J. Thornton, Conformational changes observed in enzyme crystal structures upon substrate binding, J. Mol. Biol. 346 (2005) 21–28.
[46] G.M. Lee, C.S. Craik, Trapping moving targets with small molecules, Science 324 (2009) 213–215.
[47] J.F. Swain, L.M. Gierasch, The changing landscape of protein allostery, Curr. Opin. Struct. Biol. 16 (2006) 102–108.
[48] N. Tokuriki, D.S. Tawfik, Protein dynamism and evolvability, Science 324 (2009) 203–207.
[49] V.J. Vinson, Proteins in motion. Introduction, Science 324 (2009) 197.